Performances of three models in predicting packing densities and optimal mixing fractions of mixtures of micropowders with different sizes

Wenchao Du [a], Ming Li [a], Zhijian Pei [a], and Chao Ma [a, b,*]

[a] Department of Industrial & Systems Engineering, Texas A&M University, College Station, TX 77843

[b] Department of Engineering Technology & Industrial Distribution, Texas A&M University, College Station, TX 77843

Abstract

Mixing powders with different sizes is a common method to tune the packing density. For the first time, predicted packing density and optimal mixing fraction from different linear packing models (de Larrard's, Kwan's, and Yu's) are compared against the experimental results of mixtures of micropowders (with different particle sizes: 2, 10, and 70 μm). Regarding the predicted packing density, Kwan's model achieved the smallest prediction deviations for three mixing systems of 10 μm and 2 μm powders, 70 μm and 10 μm powders, and 70 μm, 10 μm, and 2 μm powders, while de Larrard's model achieved the smallest prediction deviation for the mixing system of 70 μm and 2 μm powders. Overall for the predicted packing density, Kwan's model achieved the best prediction performance with the lowest average mean absolute error of 2.2%. Regarding the predicted optimal mixing fraction, Kwan's model outperformed the other two models for the mixing system of 10 μm and 2 μm powders and the mixing system of 70 μm and 2 μm powders, while Yu's model outperformed the other two models for the mixing system of 70 μm and 10 μm powders. Possible reasons of the better performances of Kwan's model in both prediction aspects include the consideration of wedging effect.

Keywords: mixing, powder, packing density, fraction

* Corresponding author: cma@tamu.edu

1 Introduction

Mixing powders with different sizes is a common method to tune the packing density. By controlling the particle sizes and mixing fractions of component powders, the powder mixtures can achieve different packing densities. Consequently, this method can be useful in various applications, such as to increase the powder bed density in additive manufacturing [1–3] and to decrease the porosity in concrete mixtures in construction engineering [4,5]. Instead of a trial and error approach to finding the mixing fractions to achieve the peak packing density or a specific packing density, analytical models have been developed to predict the packing density of a powder mixture using certain information such as the size, fraction, and packing density of each component powder [6,7]. The original linear packing model was proposed by Stovall et al. [8]. Several enhanced linear packing models, such as de Larrard's [9], Yu's [10], and Kwan's models [11,12], were developed to improve the prediction performances by accounting for different particle interaction effects.

Prediction performances of these models can be evaluated in terms of two aspects. The first is deviation of predicted density from measured density at different mixing fractions. It is commonly used in other studies [5,13] and is useful when the model is used to guide the selection of mixing fractions to achieve a specific packing density. The second is deviation of predicted optimal mixing fraction from the mixing fraction for the measured peak packing density (i.e., peak density). It is firstly proposed in this study and is useful when the model is used to guide the selection of optimal mixing fraction to achieve the peak density.

Table 1 lists two reported studies on comparing different linear packing models in the literature. Kwan et al. [5] mixed four rock powders with particle size ranges of 75–150, 150–300, 300–600, and >600 μm, and then compared model-predicted packing densities (by de Larrard's

and Yu's models) against the experimentally measured densities. Chan et al. [13] compared model-predicted packing densities (by de Larrard's, Yu's, and Kwan's models) against publicly available experimentally measured densities of binary mixtures (prepared from sand, polyethylene, and glass with sizes ranging from 74 μm to 20 mm). However, no study has been reported about comparing different linear packing models against experimentally measured densities for fine micropowders. Moreover, no study has been reported for any powder mixture about the deviation of predicted optimal mixing fraction from the mixing fraction for the measured peak density.

Table 1. Reported studies on comparing linear packing models in the literature

Model	**Material**	**Particle size**	**Application**	**Reference**
de Larrard's [9] and Yu's [10]	Rock and cement	75 μm – 1.8 mm	Construction Engineering	Kwan et al., 2009 [5]
de Larrard's [9], Yu's [10], and Kwan's [11,12]	Sand, polyethylene, and glass	74 μm – 20 mm	Not specified	Chan et al., 2014 [13]

This paper, for the first time, reports a study that compares the prediction performances of three packing models using experimental data from fine micropowders. In this paper, firstly, three linear packing models (de Larrard's model [9], Yu's model [10], and Kwan's model [11,12]) were introduced. Packing densities for various powder mixing systems at different fractions of component powders, as well as optimal mixing fractions for the peak packing density, were calculated from these models. Various mixing fractions were selected to prepare binary and ternary powder mixtures, and the packing density for each powder mixture was measured. The prediction performances of these three models were assessed against the experimental data.

2 Theoretical framework

The three enhanced packing models assessed in this study are de Larrard's model [9], Yu's model [10], and Kwan's model [11,12]. These models are based on the assumption that all component powders and powder mixtures are under the state of dense packing and composed of non-deformable particles [8,14]. In the case of a powder mixture with n components (the components are ranked such that $d_i \geq d_{i+1}$, where d_i is the diameter of the ith component), the model-predicted packing density (γ) is given by [16]:

$$\gamma = \min(\gamma_1, \gamma_2, \cdots, \gamma_i, \cdots, \gamma_n) \tag{1}$$

where γ_i is the model-predicted packing density of the powder mixture assuming the ith component is "dominant" [8]. Here a dominant component means that its particles are tightly packed against each other, while the other smaller component particles fill the voids among the dominant component particles, and the other larger component particles contact dominant particles only [5]. Moreover, all modeled packing densities in this paper are relative densities.

Adding a powder with a different size to an existing powder with a specific size can either increase or decrease its packing density. The added powder can increase the density by occupying the voids between finer particles, which is called the occupying effect [15], as illustrated in Figure 1(a), or by filling the voids between the coarser particles, which is called the filling effect, as illustrated in Figure 1(b). These two effects are included in the original linear packing model by Eq. (2) (and therefore in all three enhanced linear packing models).

The added powder can also decrease the packing density by three different effects. The first one is called wall effect of the coarse powder [12] when coarse particles disrupt the packing of fine particles at wall-like boundaries of coarse particles, as illustrated in Figure 1(a). The second

is called loosening effect of fine powder [12] when fine particles are squeezed between the coarse particles, as illustrated in Figure 1(b). The third is called wedging effect [11] when coarse particles are close to each other and the space between them is not enough for a fine particle to occupy (if fine powder is dominant, as illustrated in Figure 1(a)), or when fine particles trapped between coarse particles preventing coarse particles from contacting each other (if coarse powder is dominant, as illustrated in Figure 1(b)). All these three effects can be included in the model by using interaction functions [13]. Different interaction functions can be fitted using the experimental data.

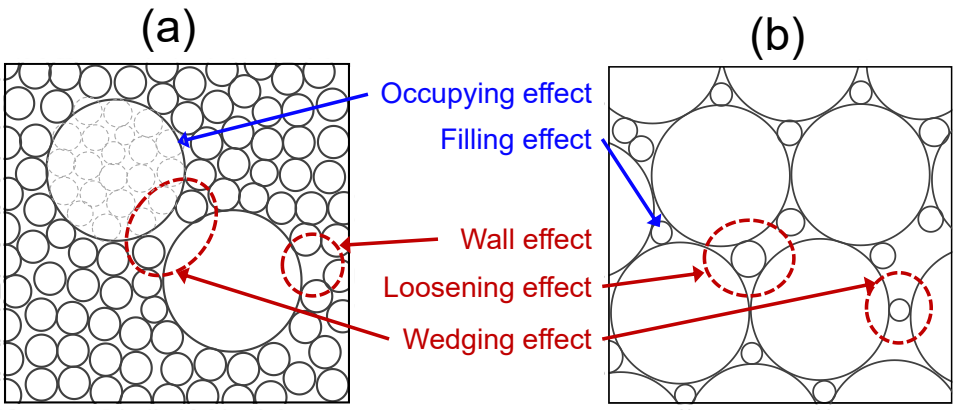

Figure 1. Illustrations of (a) occupying, wall, and wedging effects when fine powder is dominant (dashed circles in the coarse particle are imagined fine particles assuming the coarse particle is not present), and (b) filling, loosening, and wedging effects when coarse powder is dominant

In the following part of Section 2, three enhanced linear packing models are introduced. All models consider wall effect and loosening effect (by different interaction functions of these two effects). Kwan's model also considers wedging effect (by a third interaction function).

2.1 Two-parameter models (de Larrard's model and Yu's model) for both binary and ternary mixtures

A two-parameter model incorporates two effects, i.e. wall effect and loosening effect [9,10]. In a two-parameter model, the model-predicted packing density (γ_i) assuming the *i*th component is dominant is given by the following equation [5]:

$$\gamma_i = \frac{\beta_i}{1 - \sum_{j=1}^{i-1}\left[1 - \beta_i + b_{i,j}\beta_i\left(1 - \frac{1}{\beta_j}\right)\right]y_j - \sum_{j=i+1}^{n}\left[1 - a_{i,j}\frac{\beta_i}{\beta_j}\right]y_j} \tag{2}$$

where β_j and y_j are the packing density and volumetric fraction of the *j*th component, respectively. $a_{i,j}$ and $b_{i,j}$ are two interaction functions that reflect loosening and wall effects, respectively.

The interaction functions in **de Larrard's model** are [9]:

$$a_{i,j} = \sqrt{1 - \left(1 - \frac{d_j}{d_i}\right)^{1.02}} \tag{3}$$

$$b_{i,j} = 1 - \left(1 - \frac{d_j}{d_i}\right)^{1.5} \tag{4}$$

The interaction functions in **Yu's model** are [5,10]:

$$a_{i,j} = 1 - \left(1 - \frac{d_j}{d_i}\right)^{3.3} - 2.8 \cdot \frac{d_j}{d_i} \cdot \left(1 - \frac{d_j}{d_i}\right)^{2.7} \tag{5}$$

$$b_{i,j} = 1 - \left(1 - \frac{d_j}{d_i}\right)^{2} - 0.4 \cdot \frac{d_j}{d_i} \cdot \left(1 - \frac{d_j}{d_i}\right)^{3.7} \tag{6}$$

The final model-predicted packing density (γ) is determined by Eq. (1).

2.2 Three-parameter model (Kwan's model)

A three-parameter model incorporates three effects, i.e. wall effect, loosening effect, and wedging effect [11].

2.2.1 Three-parameter model for binary mixture

The model-predicted packing density, γ_i and γ_j, assuming the *i*th and *j*th component is dominant, respectively, is given by the following equations [12]:

$$\frac{1}{\gamma_i} = \left(\frac{y_i}{\beta_i} + \frac{y_j}{\beta_j}\right) - \left(1 - b_{i,j}\right)\left(1 - \beta_j\right) \cdot \frac{y_j}{\beta_j} \cdot \left[1 - c_{i,j}(2.6^{y_j} - 1)\right] \tag{7}$$

$$\frac{1}{\gamma_j} = \left(\frac{y_i}{\beta_i} + \frac{y_j}{\beta_j}\right) - \left(1 - a_{i,j}\right) \cdot \frac{y_i}{\beta_i} \cdot \left[1 - c_{i,j}(3.8^{y_j} - 1)\right] \tag{8}$$

where $a_{i,j}$, $b_{i,j}$, and $c_{i,j}$ are the interaction functions between the *i*th and *j*th component for the loosening effect, wall effect, and wedging effect, respectively. They are defined as follows [11,12]:

$$a_{i,j} = 1 - \left(1 - \frac{d_j}{d_i}\right)^{3.3} - 2.6 \cdot \frac{d_j}{d_i} \cdot \left(1 - \frac{d_j}{d_i}\right)^{3.6} \tag{9}$$

$$b_{i,j} = 1 - \left(1 - \frac{d_j}{d_i}\right)^{1.9} - 2 \cdot \frac{d_j}{d_i} \cdot \left(1 - \frac{d_j}{d_i}\right)^{6} \tag{10}$$

$$c_{i,j} = 0.322 \cdot tanh\left(11.9 \cdot \frac{d_j}{d_i}\right) \tag{11}$$

The final model-predicted packing density (γ) is determined by Eq. (1).

2.2.2 Three-parameter model for ternary mixture

When the first component (the powder with the largest particle size) is dominant, the packing density of the ternary mixture is given by the following equation [12]:

$$\frac{1}{\gamma_1}=\frac{y_1}{\beta_1}+\frac{y_2}{\beta_2}+\frac{y_3}{\beta_3}-\left(1-b_{1,2}\right)(1-\beta_2)\cdot\frac{y_2}{\beta_2}\cdot\left[1-c_{1,2}\left(2.6^{(y_2+y_3)}-1\right)\right]-\left(1-b_{1,3}\right)(1-\beta_3)\cdot\frac{y_3}{\beta_3}\cdot\left[1-c_{1,3}\left(2.6^{(y_2+y_3)}-1\right)\right] \quad (12)$$

When the second component (the powder with the intermediate particle size) is dominant, the packing density of the ternary mixture is given by the following equation [12]:

$$\frac{1}{\gamma_2}=\frac{y_1}{\beta_1}+\frac{y_2}{\beta_2}+\frac{y_3}{\beta_3}-\left(1-a_{1,2}\right)\cdot\frac{y_1}{\beta_1}\cdot\left[1-c_{1,2}(3.8^{y_1}-1)\right]-\left(1-b_{2,3}\right)(1-\beta_3)\cdot\frac{y_3}{\beta_3}\cdot\left[1-c_{2,3}(2.6^{y_3}-1)\right] \quad (13)$$

When the third component (the powder with the smallest particle size) is dominant, the packing density of the ternary mixture is given by the following equation [12]:

$$\frac{1}{\gamma_3}=\frac{y_1}{\beta_1}+\frac{y_2}{\beta_2}+\frac{y_3}{\beta_3}-\left(1-a_{1,3}\right)\cdot\frac{y_1}{\beta_1}\cdot\left[1-c_{1,3}(3.8^{y_1}-1)\right]-\left(1-a_{2,3}\right)\cdot\frac{y_2}{\beta_2}\cdot\left[1-c_{2,3}(3.8^{y_2}-1)\right] \quad (14)$$

The interaction functions are the same as Eqs. (9)–(11), and the final model-predicted packing density (γ) is given by Eq. (1).

3 Experimental method

3.1 Characterization of particle morphology

Three alumina powders with nominal particle sizes of 2, 10, and 70 μm, respectively, were purchased from Inframat Corporation and used as component powders in this study. Particle morphologies of these component powders were characterized by scanning electron microscopy (SEM, TESCAN VEGA II LSU, Brno-Kohoutovice, Czech), and are shown in Figure 2. The shapes of powder particles are primarily spherical. The particle size within each powder is not perfectly uniform, but the size variation is much smaller than the size differences across the three powders. This study focuses on spherical powders since they have been used in various

applications such as additive manufacturing [1]. Non-spherical powders will be studied in a future study.

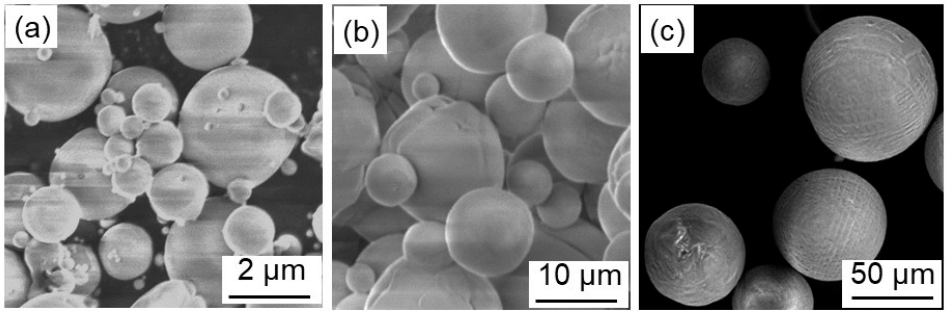

Figure 2. Particle morphologies of component powders: (a) 2 μm, (b) 10 μm, and (c) 70 μm

3.2 Preparation of powder mixtures

Three binary mixing systems and one ternary mixing system were prepared from the three component powders with sizes of 2, 10, and 70 μm. These mixing systems are denoted by 10/2, 70/2, 70/10, and 70/10/2 in this study. Various mixing fractions were selected to prepare different powder mixtures for each mixing system. All mixing fractions in this paper are based on the true (solid) volume of each powder. Since all component powders are composed of the same material (i.e., alumina), volumetric fractions are the same as mass fractions. A scale with an accuracy of 0.1 mg (AGCN200, Torbal, Oradell, NJ) was used to measure the fraction of each component powder. Measured component powders were mixed by ball milling (Jar Rolling Mills, Paul O. Abbe, Wood Dale, IL) for 1 h, using alumina balls with a diameter of 2 mm. The amount of balls was 10% of the powder mixture by mass. A low milling speed (~60 RPM) was used.

3.3 Measurement of tap density

The packing density of all component powders and powder mixtures is evaluated by tap density, a good estimation for the packing density of a densely packed powder [16,17]. The tap

density of each powder was measured by a tap density meter (DY-100A, HongTuo, Dongguan, Guangdong, China) following an ASTM standard [18]. Specifically, the mass of each powder for tap density measurement was 100 g. Each measurement included 3000 tapping cycles with a 3-mm stroke. After tapping, the absolute tap density was calculated by dividing the mass by the volume of the powder inside the cylinder. The absolute tap density was then divided by the theoretical density of alumina (3.97 g/cm^3 [19]) to obtain the relative tap density. All experimentally measured packing densities in this paper are relative tap densities. The tap densities of component powders of 2, 10, and 70 μm are 61.0%, 61.0%, and 62.2%, respectively.

4 Results and discussion

4.1 Experimental and modeling results

Experimentally measured densities and model-predicted densities from the three enhanced linear packing models for the three binary mixing systems are presented in Table 2 and Figure 3. As shown in Figure 3, the increase in the coarse powder fraction initially increased and then decreased the packing density of the powder mixtures. The increase in the fine powder fraction also initially increased and then decreased the packing density of the powder mixtures. The general trends of the relation between packing density and mixing fraction from the experiments well match those from the models.

Table 2. Experimentally measured and model-predicted packing densities for three binary mixing systems

Binary mixing system	Fraction of 2 μm powder (vol.%)	Fraction of 10 μm powder (vol.%)	Fraction of 70 μm powder (vol.%)	Packing density from experiments (%)	Packing density from de Larrard's model (%)	Packing density from Yu's model (%)	Packing density from Kwan's model (%)
10/2	53.7	46.3	/	68.7	65.1	70.0	69.4
10/2	43.7	56.3	/	70.0	66.1	72.3	71.6
10/2	33.7	66.3	/	71.0	69.0	74.8	73.9
10/2	28.7	71.3	/	71.4	71.0	72.4	75.1
10/2	23.7	76.3	/	71.6	71.4	70.1	74.9
10/2	18.3	81.3	/	69.4	70.0	68.0	71.5
10/2	13.7	86.3	/	67.1	65.7	65.9	68.3
70/2	50.0	/	50.0	74.5	73.7	75.0	74.9
70/2	40.0	/	60.0	77.6	75.8	78.6	78.5
70/2	30.0	/	70.0	80.8	78.2	82.6	82.5
70/2	25.0	/	75.0	81.1	78.5	78.4	82.4
70/2	20.0	/	80.0	76.6	74.7	74.5	77.4
70/2	15.0	/	85.0	72.5	71.9	71.0	72.9
70/2	10.0	/	90.0	68.8	66.1	67.8	69.0
70/10	/	52.3	47.7	70.5	68.6	71.7	71.3
70/10	/	42.3	57.7	72.1	72.6	74.5	73.9
70/10	/	32.3	67.7	73.5	76.3	77.4	76.8
70/10	/	27.3	77.7	74.0	76.4	74.6	78.3
70/10	/	22.3	77.7	74.2	74.0	72.0	77.0
70/10	/	17.3	82.7	71.4	70.9	69.5	73.1
70/10	/	12.3	87.7	68.7	69.0	67.2	69.6

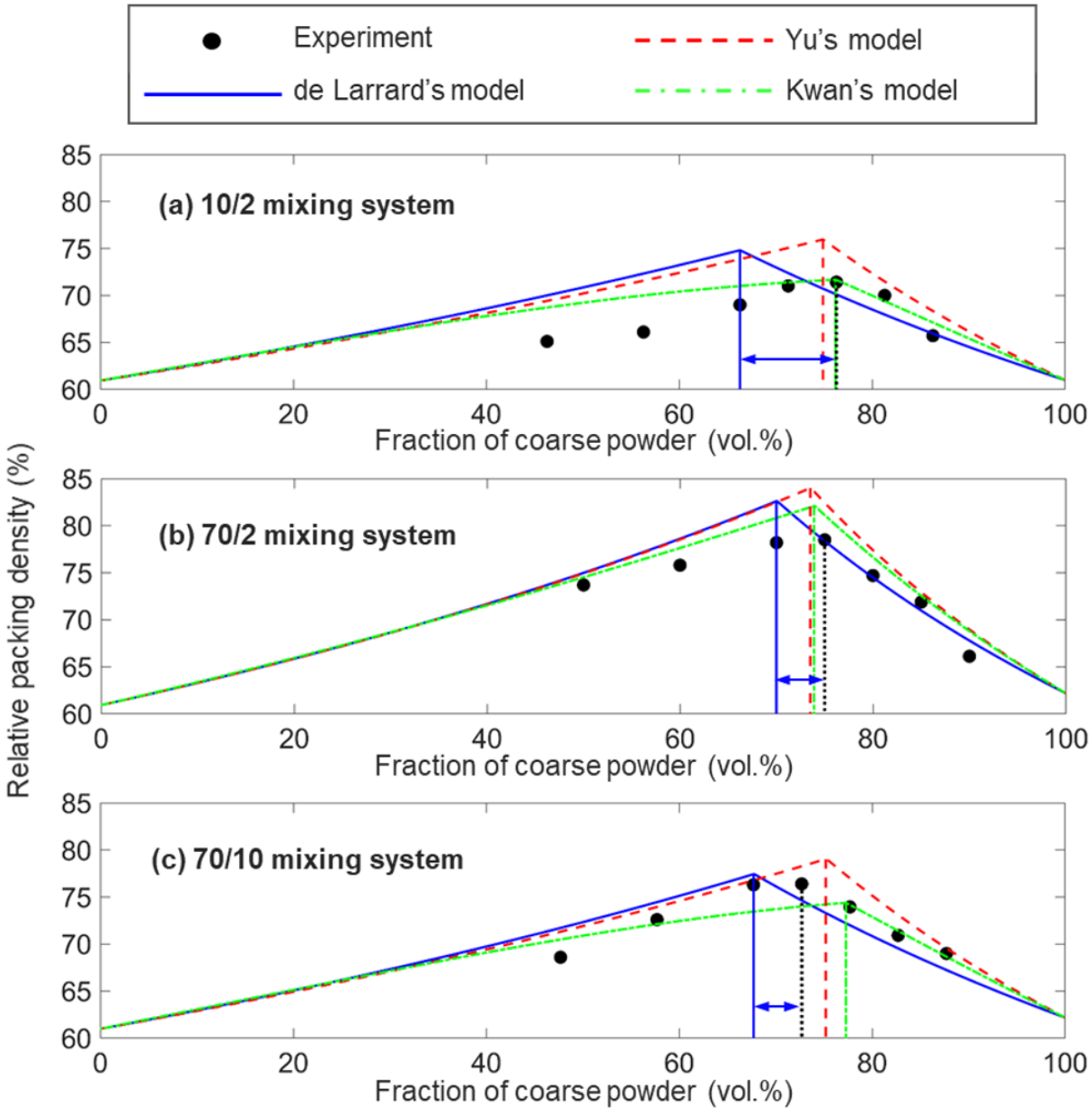

Figure 3. Experimentally measured and model-predicted packing densities for three binary mixing systems: (a) 10 μm and 2 μm powders, (b) 70 μm and 2 μm powders, and (c) 70 μm and 10 μm powders (the double arrows show the derivations of optimal mixing fraction for de Larrard's model as examples)

Experimentally measured densities and model-predicted densities from the three enhanced packing models for the ternary mixing system are presented in Table 3 and Figure 4. The method to read the ternary plot can be found in the authors' previously published paper [1]. Based on both experimental and modeling results, the highest packing density can be achieved at relatively low fractions of 2 and 10 μm powders and a relatively high fraction of 70 μm powder. The general trends of the relation between packing density and mixing fraction from the experiments well match those from the models.

Table 3. Experimentally measured and model-predicted packing densities for the ternary mixing system

Fraction of 2 μm powder (vol.%)	**Fraction of 10 μm powder (vol.%)**	**Fraction of 70 μm powder (vol.%)**	**Packing density from experiments (%)**	**Packing density from de Larrard's model (%)**	**Packing density from Yu's model (%)**	**Packing density from Kwan's model (%)**
10	10	80	74.1	72.6	76.3	75.2
10	80	10	66.7	66.7	68.4	67.8
20	20	60	78.2	84.7	84.3	80.6
20	30	50	77.7	83.1	83.0	79.0
20	40	40	76.1	79.7	81.8	77.5
20	60	20	71.1	73.7	78.0	74.5
30	20	50	79.0	80.5	80.1	77.9
30	30	40	76.4	79.5	79.0	76.4
30	40	30	76.6	78.6	77.9	75.1
40	20	40	75.3	76.7	76.4	75.1
40	30	30	73.1	75.8	75.3	73.8
40	40	20	70.8	74.9	74.3	72.7
60	20	20	67.5	70.1	69.8	69.6
80	10	10	64.4	65.2	65.1	65.2

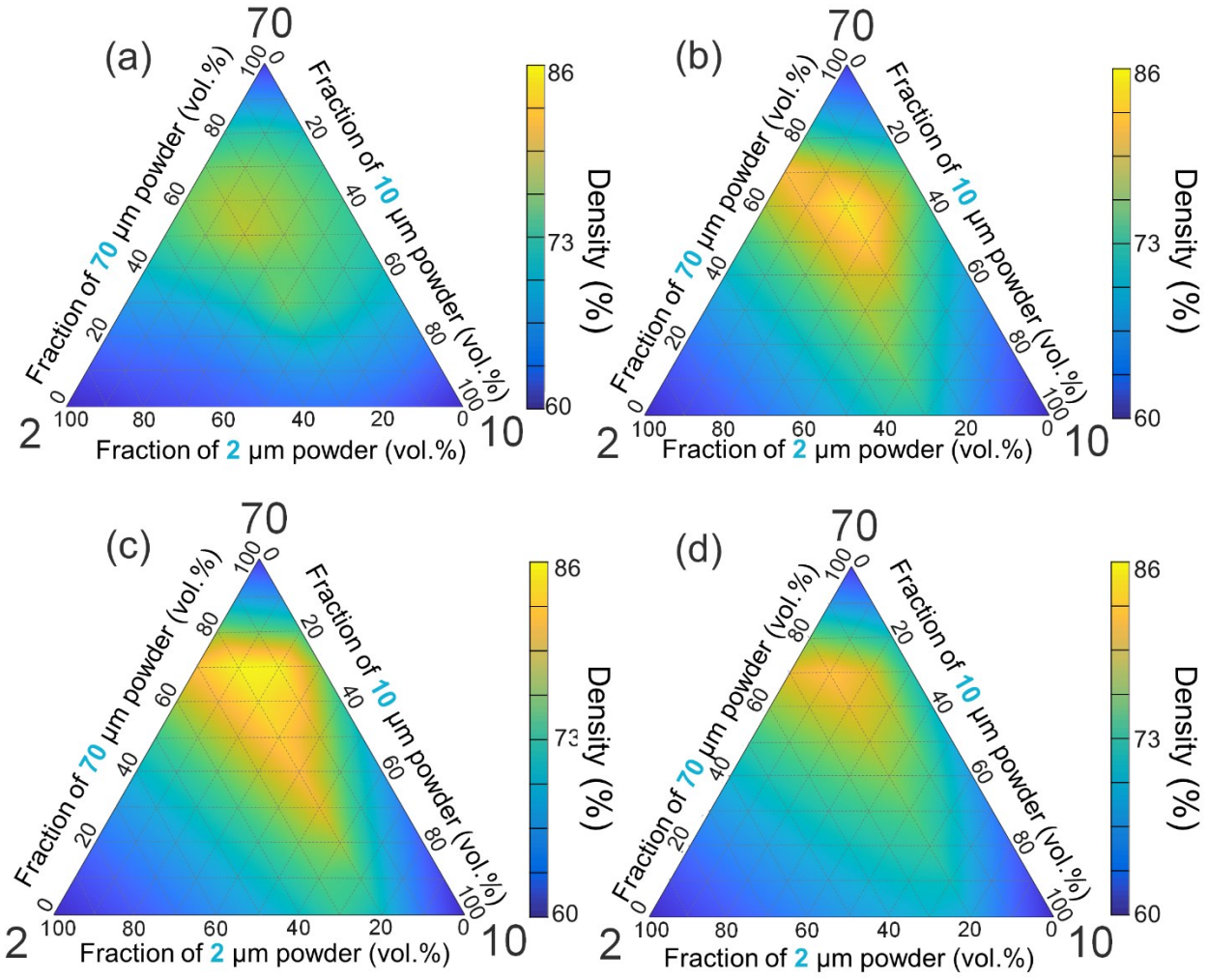

Figure 4. Packing densities for the ternary mixing system from (a) experiments, (b) de Larrard's model, (c) Yu's model, and (d) Kwan's model

4.2 Performances of three enhanced linear packing models

4.2.1 Deviation of predicted density from measured density at different mixing fractions

For a powder mixture, the deviation of predicted density from measured density (Dev_γ) at a specific mixing fraction was calculated based on the following equation:

$$Dev_\gamma = \frac{\gamma_M - \gamma_E}{\gamma_E} \tag{15}$$

where γ_M and γ_E are the model-predicted and experimentally measured packing densities, respectively.

Figures 5 and 6 show the deviations of predicted density for binary and ternary mixing systems, respectively. A positive deviation value indicates that the model-predicted density is higher than the experimentally measured one. De Larrard's model has both higher and lower predications than experimental values for all three binary mixing systems. Yu's model predictions are consistently higher than the experimental values. Kwan's model predictions are consistently higher than the experiment values for the 70/2 mixing system, but sometimes higher and sometimes lower than the experiment values for the other two mixing systems.

There are more positive deviation values than negative ones in both Figures 5 and 6, indicating that most of the model-predicted results are higher than the experimental ones. Predictions by Kwan's model (maximum deviation is 5.9%) have smaller positive deviations than those by de Larrard's and Yu's models (maximum deviations are 9.4% and 9.6%, respectively). Possible reasons include the consideration of the wedging effect in Kwan's model [11] that leads to lower density predictions (closer to the experimental results).

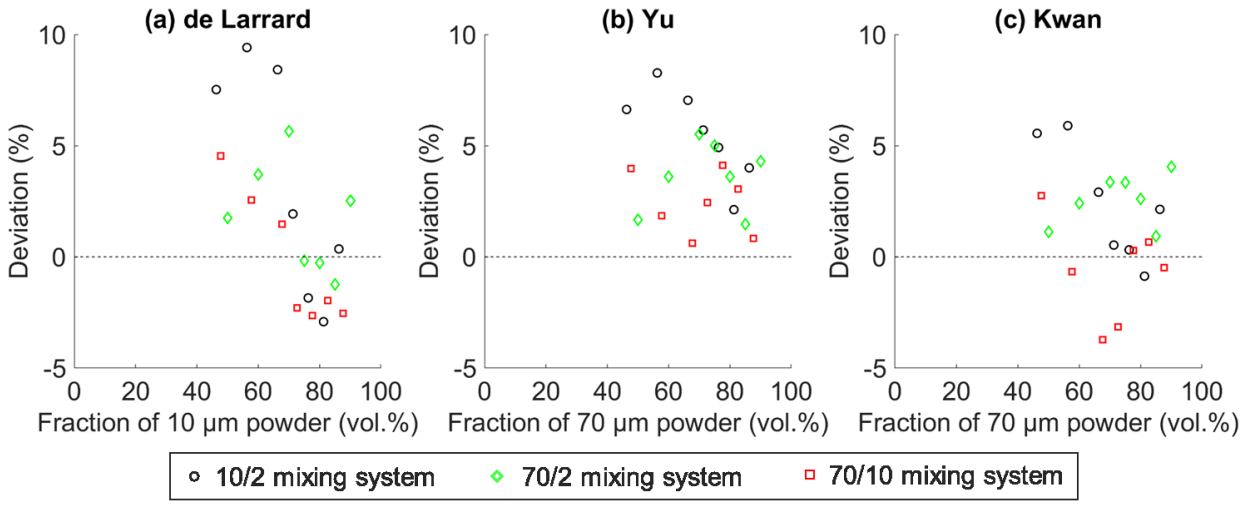

Figure 5. Deviations of predicted packing density for three binary mixing systems from three models: (a) de Larrard's, (b) Yu's, and (c) Kwan's

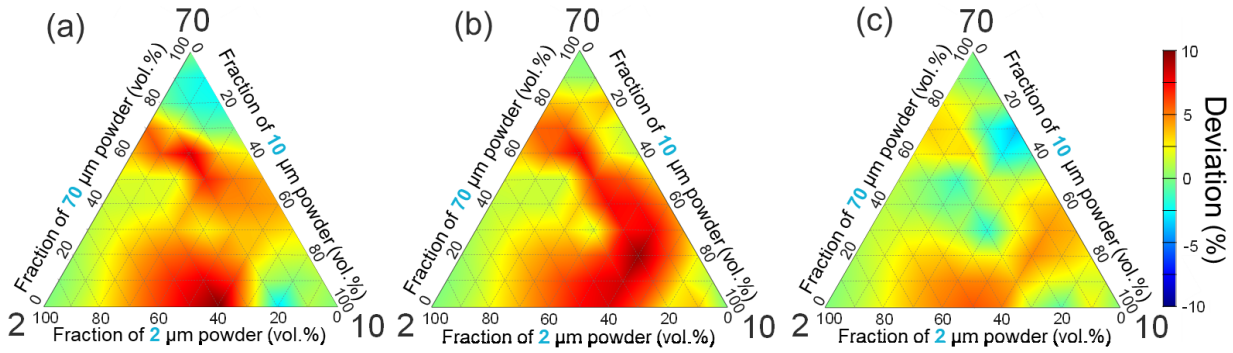

Figure 6. Deviations of predicted packing density for the ternary mixing system from three models: (a) de Larrard's, (b) Yu's, and (c) Kwan's

Mean absolute error (MAE) is a measure of the degree of deviation [20]. It was used in this study to evaluate the overall deviation of a model for a mixing system. For a specific model (i.e., de Larrard's, Yu's, or Kwan's), its MAE (e) for a mixing system (i.e., $e_{10/2}$, $e_{70/2}$, $e_{70/10}$, or $e_{70/10/2}$) is given by:

$$e = \frac{\sum_{i=1}^{n} \left| \gamma_{M_i} - \gamma_{E_i} \right|}{n} \tag{16}$$

where γ_{M_i} is the model-predicted density and γ_{E_i} is the experimentally measured density of the *i*th powder mixture. Here *n* is the number of powder mixtures in the corresponding mixing system that were experimentally studied (i.e., the number of rows in Tables 2 and 3 for each mixing system).

To evaluate the overall performance of a specific model considering all mixing systems, the average MAE (e_{avg}) of packing density for each model was calculated based on the MAE values of all four mixing systems, which was given by:

$$e_{avg} = \frac{e_{10/2} + e_{70/2} + e_{70/10} + e_{70/10/2}}{4} \tag{17}$$

The MAE values from Eq. (16) and Eq. (17) are shown in Table 4. Kwan's model has the smallest MAE values of 2.6%, 1.7%, and 1.8% for the mixing systems of 10/2, 70/10, and 70/10/2, respectively. For the mixing system of 70/2, Yu's model has the smallest MAE value of 2.2%. Overall, Kwan's model has the smallest average MAE of 2.2% among all three models.

Table 4. Mean absolute error (MAE, e) values of packing density for three enhanced linear packing models for different mixing systems

Mixing system	**MAE of packing density for de Larrard's model (%)**	**MAE of packing density for Yu's model (%)**	**MAE of packing density for Kwan's model (%)**
10/2	4.6	5.5	2.6
70/2	2.2	3.6	2.6
70/10	2.6	2.4	1.7
70/10/2	3.8	4.2	1.8
Average	3.3	3.9	2.2

4.2.2 Deviation of predicted optimal mixing fraction from the mixing fraction for the measured peak density

In this section, the deviation of predicted optimal mixing fraction for all three binary mixing systems is calculated. For a mixing system, the deviation of predicted optimal mixing fraction was determined by the following equation:

$$Dev_y = y_M - y_E \tag{18}$$

where y_M and y_E are the model-predicted and experimentally determined values of optimal mixing fraction of the coarse powder corresponding to the peak density, respectively. In each subfigure of Figure 3, the black vertical line corresponds to the value of y_E, and the other three vertical lines correspond to three values of y_M for three models, respectively. In each subfigure, the blue vertical line (i.e., model-predicted optimal mixing fraction by de Larrard's model) is always the furthest from the black vertical line (i.e., experimentally determined optimal mixing fraction), meaning that de Larrard's model has the largest absolute deviation values. The double arrows show the deviations of optimal mixing fraction (i.e., Dev_y) for de Larrard's model as examples.

Table 5 lists the model-predicted optimal mixing fractions from all three models and the corresponding experimental results for the three binary mixing systems. Figure 7 illustrates deviations of model-predicted optimal mixing fraction for all three binary mixing systems. Positive and negative deviation values mean larger and smaller model-predicted optimal mixing fractions than the optimal mixing fraction for the measured peak density, respectively. For binary mixing systems of 10/2 and 70/2, all three models underpredicted the optimal mixing fractions of the coarse powder. For the binary mixing system of 70/10, de Larrard's model underpredicted the optimal mixing fraction of the coarse powder and the other two models overpredicted it.

For assessing performances of different models in terms of optimal mixing fraction, the absolute values of deviations calculated from Eq. (18), i.e., $|Dev_y|$, were compared. Consequently, it was found that Kwan's model outperformed the other two models for mixing systems of 10/2 and 70/2, and Yu's model outperformed the other two models for the mixing system of 70/10.

Table 5. Optimal mixing fractions of the coarse powder from models and experiments for three binary mixing systems

Binary mixing system	Optimal mixing fraction from de Larrard's model (%)	Optimal mixing fraction from Yu's model (%)	Optimal mixing fraction from Kwan's model (%)	Optimal mixing fraction from experiments (%)
10/2	66.3	74.9	76.2	76.3
70/2	67.7	75.2	77.3	72.7
70/10	70.0	73.5	73.9	75.0

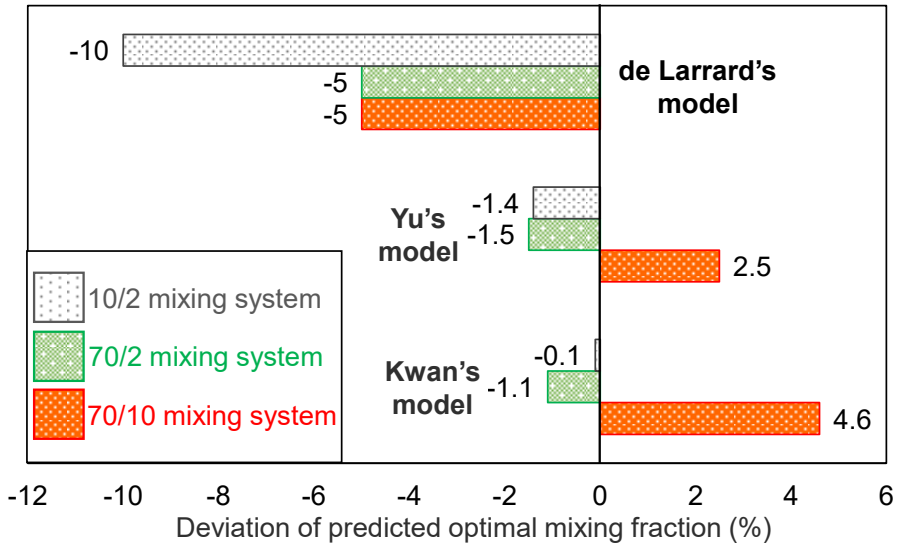

Figure 7. Deviations of model-predicted optimal mixing fraction of the coarse powder from the mixing fraction for the measured peak density of three binary mixing systems

5 Conclusions

This paper assessed the performances of three enhanced linear packing models in predicting packing densities and optimal mixing fractions of mixtures of micropowders with different sizes down to 2 μm. The results on deviation of predicted packing density showed that Kwan's model achieved the smallest prediction deviations for three mixing systems of 10 μm and 2 μm powders, 70 μm and 10 μm powders, and 70 μm, 10 μm, and 2 μm powders, while de Larrard's model achieved the smallest prediction deviation for the mixing system of 70 μm and 2 μm powders. Kwan's model achieved the best overall prediction performance (with an average mean absolute error of 2.2%) among all three models on deviation of predicted packing density. The results on deviation of predicted optimal mixing fraction showed that Kwan's model outperformed the other two models for the mixing system of 10 and 2 μm powders (with a deviation value of -0.1%) and the mixing system of 70 and 2 μm powders (with a deviation value of -1.1%), and that Yu's model outperformed the other two models for the mixing system of 70 and10 μm powders (with a deviation value of 2.5%). This assessment study of prediction performances of three linear packing models provides a guidance for preparing micropowder mixtures.

Acknowledgements

This material is based upon work supported by the National Science Foundation under Grant No. 1762341 (Division of Civil, Mechanical and Manufacturing Innovation).

References

[1] W. Du, J. Roa, J. Hong, Y. Liu, Z. Pei, C. Ma, Binder Jetting Additive Manufacturing: Effect of Particle Size Distribution on Density, Journal of Manufacturing Science and Engineering. 143 (2021) 091002 (9 pages). https://doi.org/10.1115/1.4050306.

[2] Y. Bai, G. Wagner, C.B. Williams, Effect of Particle Size Distribution on Powder Packing and Sintering in Binder Jetting Additive Manufacturing of Metals, Journal of Materials Science and Engineering. 139 (2017) 081019 (6 pages). https://doi.org/10.1017/CBO9781107415324.004.

[3] W. Du, X. Ren, Z. Pei, C. Ma, Ceramic binder jetting additive manufacturing: A Literature review on density, Journal of Manufacturing Science and Engineering. 142 (2020) 040801 (19 pages). https://doi.org/10.1115/1.4046248.

[4] A.K.H. Kwan, V. Wong, W.W.S. Fung, A 3-parameter packing density model for angular rock aggregate particles, Powder Technology. 274 (2015) 154–162. https://doi.org/10.1016/j.powtec.2014.12.054.

[5] A.K.H. Kwan, W.W.S. Fung, Packing density measurement and modelling of fine aggregate and mortar, Cement and Concrete Composites. 31 (2009) 349–357. https://doi.org/10.1016/j.cemconcomp.2009.03.006.

[6] W. Du, X. Ren, Y. Chen, C. Ma, M. Radovic, Z. Pei, Model guided mixing of ceramic powders with graded particle sizes in binder jetting additive manufacturing, in: ASME 2018 13th International Manufacturing Science and Engineering Conference, College Station, TX, 2018: p. V001T01A014 (9 pages). https://doi.org/https://doi.org/10.1115/MSEC2018-6651.

[7] C.C. Furnasz, Grading Aggregates I-Mathematical Relations for Beds of Broken Solids of Maximum Density, Industrial & Engineering Chemistry. 23 (1931) 1052–1058.

[8] T. Stovall, F. de Larrard, M. Buil, Linear packing density model of grain mixtures, Powder Technology. 48 (1986) 1–12. https://doi.org/10.1016/0032-5910(86)80058-4.

[9] F. de Larrard, Concrete mixture proportioning: a scientific approach, E & FN Spon, London, 1999.

[10] A.B. Yu, R.P. Zou, N. Standish, Modifying the linear packing model for predicting the porosity of nonspherical particle mixtures, Industrial & Engineering Chemistry Research. 35 (1996) 3730–3741. https://doi.org/10.1021/ie950616a.

[11] A.K.H. Kwan, K.W. Chan, V. Wong, A 3-parameter particle packing model incorporating the wedging effect, Powder Technology. 237 (2013) 172–179. https://doi.org/10.1016/j.powtec.2013.01.043.

[12] V. Wong, A.K.H. Kwan, A 3-parameter model for packing density prediction of ternary mixes of spherical particles, Powder Technology. 268 (2014) 357–367. https://doi.org/10.1016/j.powtec.2014.08.036.

[13] K.W. Chan, A.K.H. Kwan, Evaluation of particle packing models by comparing with published test results, Particuology. 16 (2014) 108–115. https://doi.org/10.1016/j.partic.2013.11.008.

[14] W. Du, M. Singh, D. Singh, Binder jetting additive manufacturing of silicon carbide ceramics: Development of bimodal powder feedstocks by modeling and experimental methods, Ceramics International. 46 (2020) 19701–19707. https://doi.org/10.1016/j.ceramint.2020.04.098.

[15] H.H.C. Wong, A.K.H. Kwan, Packing density of cementitious materials: part 1—measurement using a wet packing method, Materials and Structures. 41 (2008) 689–701. https://doi.org/10.1617/s11527-007-9274-5.

[16] A.B. Yu, J. Bridgwater, A. Burbidge, On the modelling of the packing of fine particles, Powder Technology. 92 (1997) 185–194. https://doi.org/10.1016/S0032-5910(97)03219-1.

[17] E.C. Abdullah, D. Geldart, The use of bulk density measurements as flowability indicators, Powder Technology. 102 (1999) 151–165. https://doi.org/10.1016/S0032-5910(98)00208-3.

[18] ASTM International, B527-15: Standard Test Method for Tap Density of Metal Powders and Compounds, (2015).

[19] M.N. Rahaman, Ceramic processing and sintering, 2nd ed., CRC Press, New York, 2003.

[20] C. Willmott, K. Matsuura, Advantages of the mean absolute error (MAE) over the root mean square error (RMSE) in assessing average model performance, Climate Research. 30 (2005) 79–82. https://doi.org/10.3354/cr030079.

List of Table Captions

List of Figure Captions

Figure 6. Deviations of predicted packing density for the ternary mixing system from three models: (a) de Larrard's, (b) Yu's, and (c) Kwan's

Figure 7. Deviations of model-predicted optimal mixing fraction of the coarse powder from the mixing fraction for the measured peak density of three binary mixing systems